A Parameterized Surface Reflectivity Model and Estimation of Bare-Surface Soil Moisture With L-Band Radiometer

Jiancheng Shi, *Senior Member, IEEE*, K. S. Chen, *Senior Member, IEEE*, Qin Li, Thomas J. Jackson, *Fellow, IEEE*, Peggy E. O'Neill, and Leung Tsang, *Fellow, IEEE*

***Abstract*—Soil moisture is an important parameter for hydrological and climatic investigations. Future satellite missions with L-band passive microwave radiometers will significantly increase the capability of monitoring earth's soil moisture globally. Understanding the effects of surface roughness on microwave emission and developing quantitative bare-surface soil moisture retrieval algorithms is one of the essential components in many applications of geophysical properties in the complex earth terrain by microwave remote sensing. In this study, we explore the use of the integral equation model (IEM) for modeling microwave emission. This model was validated using a three-dimensional Monte Carlo model. The results indicate that the IEM model can be used to simulate the surface emission quite well for a wide range of surface roughness conditions with high confidence. Several important characteristics of the effects of surface roughness on radiometer emission signals at L-band 1.4 GHz that have not been adequately addressed in the current semiempirical surface effective reflectivity models are demonstrated by using IEM-simulated data. Using an IEM-simulated database for a wide range of surface soil moisture and roughness properties, we developed a parameterized surface effective reflectivity model with three typically used correlation functions and an inversion model that puts different weights on the polarization measurements to minimize surface roughness effects and to estimate the surface dielectric properties directly from dual-polarization measurements. The inversion technique was validated with four years (1979–1982) of ground microwave radiometer experiment data over several bare-surface test sites at Beltsville, MD. The accuracies in random-mean-square error are within or about 3% for incidence angles from 20° to 50°.**

***Index Terms*—L-band radiometer, soil moisture, surface emission.**

I. Introduction

SOIL MOISTURE is a key parameter in numerous environmental studies, including hydrology, meteorology, and agriculture. Previous investigations have established the fundamentals of passive microwave remote sensing as an important tool in determining the physical properties of soils [1]–[8]. The ability to estimate soil moisture in the surface layer to an approximately 5-cm depth by microwave remote sensing at 1.4 GHz has been demonstrated under a variety of topographic and land cover conditions. Application of microwave retrieval of soil moisture to hydrological and meteorological sciences has been influenced by the natural variability and complexity of the vegetation canopy and surface roughness that significantly affect the sensitivity of emission measurements to soil moisture. At high frequencies (C-band or higher), it is well understood that the instrument's ability to monitor soil moisture is limited by vegetation cover. At lower frequencies, this problem can be greatly reduced. Two possible future spaceborne L-band multipolarization passive microwave techniques—two-dimensional synthetic aperture interferometry [5], [8] and filled-aperture mesh deployable reflectors [9]—will significantly increase the capability of monitoring earth's soil moisture globally. In addition to operating at long wavelengths, these multipolarization instruments provide an opportunity to utilize multiple polarization data in the estimation of soil moisture. The full utilization of these data will require a further understanding of surface roughness effects on the emission signals, especially on the relationships of the emission signals at different polarizations, in order to develop a quantitative algorithm for global soil moisture mapping.

The surface reflectivity model is one of the essential components in many applications of microwave remote sensing of geophysical properties in complex earth terrain. It is a direct component in monitoring soil moisture in bare or vegetated surfaces and serves as the boundary condition in studying snow, vegetation, and atmospheric properties. Currently, there are two types of approaches used to model surface reflectivity:

1) *semiempirical approach:* this type of model is generally found to be easy to use without significant computing efforts and is generally easy to implement as an inversion model;
2) *physical modeling approach:* the surface reflectivity can be obtained by integrating the bistatic scattering coefficient over the upper hemisphere [10].

The most commonly used semiempirical model that describes the bare-surface emission as a function of the surface roughness and dielectric properties is the so-called Q/H model [11], [12]. The parameter Q describes the energy emitted in orthogonal po-

Manuscript received July 10, 2002; revised September 13, 2002.

J. Shi is with the Institute for Computational Earth System Sciences, University of California, Santa Barbara, CA 93106 USA (e-mail: shi@icess.ucsb.edu).

K. S. Chen is with the Center for Space and Remote Sensing Research, National Central University, Chung-Li, Taiwan 32054.

Q. Li is with the Department of Electrical Engineering, University of Washington, Seattle, WA 98195 USA.

T. J. Jackson is with the Agricultural Research Service Hydrology and Remote Sensing Laboratory, U.S. Department of Agriculture, Beltsville, MD 20705 USA (e-mail: tjackson@hydrolab.arsusda.gov).

P. E. O'Neill is with the NASA Goddard Space Flight Center, Greenbelt, MD 20771 USA.

L. Tsang was with the University of Washington, Seattle, WA USA. He is now with the Department of Electronic Engineering, the City University of Hong Kong, Hong Kong, China.

Digital Object Identifier 10.1109/TGRS.2002.807003

larizations due to surface roughness effects. H is a measure of the effect of surface roughness to increase surface emissivity. However, it has been recognized that there can be a great difference between the direct physical measurements of surface roughness in the field and those derived by fitting the Q/H model with observed soil moisture or dielectric constant measurements [13], [14]. Commonly, the surface roughness parameter in the Q/H model has to be determined empirically from the experiment data and often is called "effective roughness." This is an inconvenient technique to apply in either the forward calculation to relate the soil moisture with microwave radiometer measurements or the inverse calculation, since there are no quantitative relationships between the empirical roughness parameter and the commonly used measurable surface roughness characteristics such as the root-mean-square (rms) height s, the autocorrelation length l, and the autocorrelation function.

Attempts to improve understanding of the effects of surface roughness and how traditional surface roughness parameters can be directly related to emission signals have resulted in the development of several surface reflectivity models. In comparison with the Q/H model, all of these models determined that the Q parameter is not very important [14]–[17]. Depending on the empirical data sources and the techniques used to develop the reflectivity models, the H parameter can have a variety of different forms.

- Mo and Schmugge [15] simulated the effects of surface roughness on the effective surface reflectivity using the Kirchhoff model and compared L- and C-band measurements from three field sites with different roughness conditions. They found that the H parameter depends on soil moisture and the ratio of s/l and that it varies with the incidence angle and polarization.
- Saatchi *et al.* [16] used the traditional surface scattering models—small perturbation model, physical optical model, and geometric optical model—to simulate the effect of surface roughness for horizontal (H) polarization and compared the results with experimental data over a frequency range of 1–12 GHz. A parameterized reflectivity model was developed with two (coherent and noncoherent) components. Unfortunately, vertical (V) polarization was not studied.
- Wegmüller and Mätzler [14] developed an empirical rough-surface reflectivity model using ground radiometer measurements with frequencies ranging from 1–100 GHz and with incidence angles of 20° to 70°. The reported accuracies of the surface reflectivity in terms of the random-mean-square errors (rmse) were 0.095 and 0.061 for H and V polarizations, respectively. This level of accuracy is about 20% of the dynamic range of the surface emission response to soil moisture.
- Wigneron *et al.* [17] also developed an empirical rough-surface reflectivity model using experimental measurements over seven different roughness conditions at L-band 1.4 GHz and incidence angles $\leq 40^{\circ}$. The reported accuracy for the surface reflectivity was 0.031 (rmse). This study concluded that the H parameter is independent of both incidence angle and polarization.

These simplified semiempirical approaches have generally focused on evaluating the magnitude of the relationship between the emission signals and the surface roughness. They are useful for the quick evaluation of the impact of roughness on surface emissions, but they do not have sufficient accuracy for the forward calculation of surface emissivity due to the nature of the semiempirical approach—i.e., limited observations and uncertainties in both instrument and field measurements. The common weakness of these semiempirical models [14], [15], [17] is that they all incorrectly presented the relationships between V and H polarizations, since they all assumed that the effects of surface roughness on emissions at different polarizations had the same magnitude and direction (increase or decrease the surface effective reflectivity) for any given surface roughness properties. For instance, the models developed in [15] and [17] showed that the V/H ratio of the surface effective reflectivity would be independent of the surface roughness and only dependent on the Fresnel reflectivity ratio. In other words, it only depends upon the surface dielectric or moisture properties. The model in [14] showed that this ratio is independent of both the surface roughness and dielectric properties. This is a quite misleading concept, and we will demonstrate in Section III that surface roughness has a significant impact on the V/H ratio measurements.

Theoretical modeling efforts have also significantly improved in recent years. The limitations of the commonly used models—small perturbation model, physical optical model, and geometric optical model—have been recognized, especially where each model can be applied to certain roughness conditions [10] and the fact that many natural surfaces are located outside of the applicable roughness ranges of these models [18]. In numerical simulation, a three-dimensional (3-D) Monte Carlo model has been developed [19], [20]. It solves Maxwell equations directly and allows the computation of the surface reflectivity without any approximation. In analytical model developments, the integral equation model (IEM) has demonstrated a much wider application range for surface roughness conditions [21]. Recently, a physically based transition function has been developed and implemented as part of the IEM model. This transition function improves the calculation of Fresnel reflection coefficients in the IEM model and connects the backscattering and emission over a wide range of surface roughness conditions [22]. Comparison with experiment data [18] showed a significant improvement in accuracy. These recent advances in theoretical models now allow more accurate calculation of surface reflectivity. Although the IEM model is valid for a wider range of surface roughness conditions when compared to other early theoretical models, the complexity of this model makes direct application using microwave radiometer data to infer soil moisture and roughness parameters rather difficult. Therefore, there is a need to develop a simple yet accurate surface reflectivity model.

Furthermore, a technique that estimates bare-surface soil moisture directly using emission signal measurements has yet to be developed. The currently used single-frequency inversion technique [1], [2] requires surface roughness ancillary data to correct for the effect of surface roughness. In this study, we use data simulated by the IEM model [22] to evaluate the use

TABLE I
SUMMARY OF THE SURFACE ROUGHNESS PARAMETERS, PERMITTIVITIES USED IN MONTE CARLO SIMULATION. THE PARAMETERS IN THE TOP TABLE WITH DIFFERENT COMBINATIONS WERE USED TO SIMULATE EMISSIVITY AT BOTH 40° AND 50°. THE OTHER FIVE PAIRS OF THE SURFACE ROUGHNESS PARAMETERS WITH EIGHT PERMITTIVITIES SHOWN IN THE BOTTOM OF THE TABLE WERE SIMULATED AT 50° ONLY

rms height (λ)	0.05	0.10	0.15						
Correlation length (λ)	0.33	0.40	0.50	0.60	0.70	0.80	0.90	1.00	
Relative Permittivity	4.06 + i0.300	4.81 + i0.45	5.56 + i0.600	7.35 + i0.872	10.8 + i1.335	14.25 + i1.797	17.7 + i2.260	21.15 + i2.722	24.6 + i3.185

Pairs of rms height (λ) & Correlation length (λ)	035 & 0.17	0.12 & 0.38	0.122 & 0.58	0.3 & 1.0	0. 41 & 1.33			
Relative Permittivity	3.66 + i0.15	4.66 + i0.29	6.26 + i0.52	8.45 + i0.85	11.3 + i1.27	15.2 + i1.82	19.2 + i2.41	23.1+ i3.04

of a single-frequency (L-band) and dual-polarization (V and H) microwave radiometer in the estimation of soil moisture for bare surfaces. The objectives that will be addressed here are as follows.

- Develop a parameterized surface reflectivity model for L-band (1.4 GHz) using IEM-simulated data for a wide range of surface roughness and soil moisture conditions. This model provides a simple but accurate connection between the surface reflectivity at different polarizations and the commonly used surface roughness measurements such as s—surface rms height, l—correlation length, and the correlation functions in order to avoid intensive computational efforts.
- Demonstrate the characteristics of surface roughness effects at different polarizations and incidence angles.
- Develop a quantitative algorithm for estimating bare-surface soil moisture directly from dual-polarization measurements without requiring surface roughness ancillary data.

Section II shows the validation of the IEM model in comparison with the 3-D Monte Carlo simulated emissivity data to establish confidence in our IEM model simulations. We then demonstrate the effects of surface roughness on the emission signals at different polarizations and incidence angles in Section III and the development of a parameterized IEM model in Section IV. In Section V, we show the development of a soil moisture algorithm that uses dual polarization measurements to minimize surface roughness effects, followed by validation of the algorithm using ground-based L-band radiometer measurements over a four-year period in Section VI, and we provide conclusions in Section VII.

II. VALIDATION OF THE IEM EMISSION MODEL

Theoretical models [10], [21] to account for the effect of surface roughness on microwave emission are based on the following equation:

$$E_p(\theta) = 1 - R_p^e(\theta) = 1 - R_p^{\text{non}}(\theta) - R_p^{\text{coh}}(\theta) \qquad (1)$$

where E_p is the surface emissivity; θ is the incidence angle; R_p^e is the surface effective reflectivity, which consists of two components: the noncoherent component R_p^{non} and coherent component R_p^{coh}. R_p^{non} can be obtained by integrating the bistatic scattering coefficient σ over the upper hemisphere

$$R_p^{\text{non}} = \frac{1}{4\pi\cos\theta}\int_0^{2\pi}\int_0^{\pi/2}[\sigma_{pp}(\theta,\theta_j,\phi_j)+\sigma_{pq}(\theta,\theta_j,\phi_j)] \cdot \sin\theta_j \cdot d\theta_j \cdot d\theta_j. \qquad (2)$$

The subscript p or q describes the polarization state, and j indicates the scattering direction.

$$R_p^{\text{coh}} = r_p \cdot \exp\left[-(2\cdot ks\cdot\cos\theta)^2\right]. \qquad (3)$$

The r is the smooth-surface Fresnel reflectivity. k is the wave number in free space, and s is the standard deviation of surface height. Equation (1) is based on energy conservation that states that the nonscattered energy from the soil surface is equal to the transmitted and absorbed energy in the soil. The emitted energy is equal to the absorbed energy under thermal equilibrium conditions.

To evaluate the IEM model [22] for simulating surface emissivity at L-band for random rough surfaces, we compared the 3-D Monte Carlo simulated emissivity data at viewing angles of 40° and 50°. The Monte Carlo simulation results were computed with the sparse-matrix canonical-grid method [19] and the physics-based two-grid method [20]. The Monte Carlo simulated emissivity data cover a wide range of surface roughness and dielectric properties. The surface roughness parameters and the relative dielectric constants used in the simulations are listed in Table I. The parameters in the top table with different combinations were used to simulate emissivity at both 40° and 50°. The other five pairs of the surface roughness parameters with eight permittivities shown in the bottom of the table were simulated at 50° only. The total number of simulated cases was 216 at 40° and 256 at 50°. The surface rms height ranges from 0.035–0.41 wavelengths, and the correlation length ranges from 0.17–1.33 wavelengths. They correspond to surface rms heights of 0.74–8.6 cm at L-band 1.41 GHz and correlation lengths from 3.5–28 cm. The gauss correlation function was used in the simulation. The real part of the dielectric constant covers a range from 3.6–24.6.

Fig. 1 shows a comparison of IEM-simulated (x axis) and Monte Carlo simulated (y axis) emissivity at 40° (left) and 50° (right) for V (top) and H (bottom) polarizations. The accura-

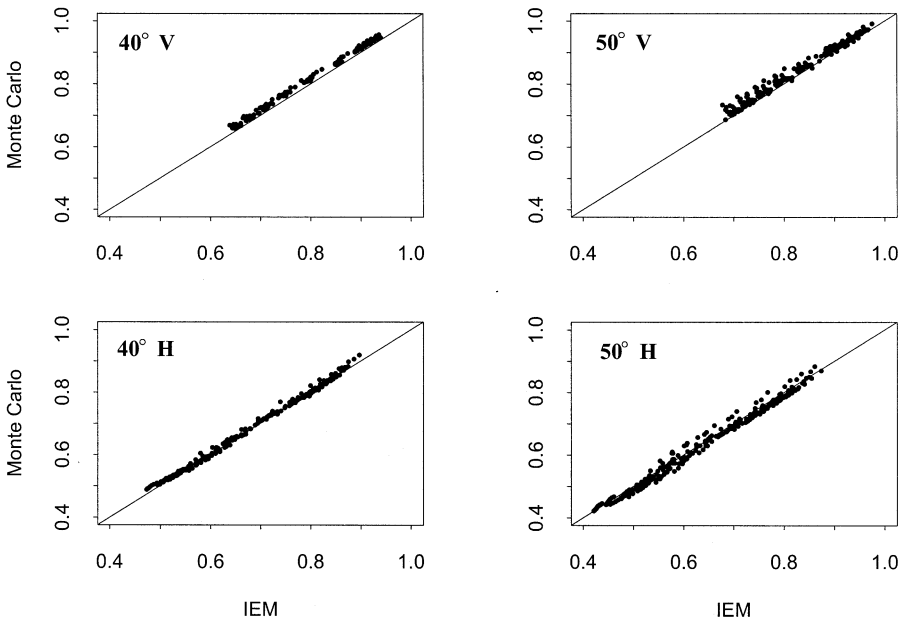

Fig. 1. Comparison of IEM model (x axis) with 3-D Monte Carlo model simulated emissivity (y axis) at 40° (left) and 50° (right) for V (top) and H (bottom) polarization.

cies at 40° in terms of rmse are 0.010 and 0.008 for V and H polarization. For V polarization, the IEM model systematically overestimates emissivity or underestimates the surface reflectivity slightly. At 50°, the rmses are 0.013 and 0.017 for V and H polarizations. Similarly, the IEM model overestimates the emissivity of V polarization in most of the cases. In terms of modeling the electromagnetic emission signal given well-characterized random rough surfaces, the results indicate that the IEM model can be used to simulate the surface emission quite well for a wide range of surface roughness conditions with high confidence.

III. Effects of Surface Roughness Properties

In order to evaluate and characterize the effects of roughness on surface emission, we generated a simulated surface emission database for L-band at 1.4 GHz and both V and H polarizations using the IEM model. This database covers a wide range of soil moisture, roughness characteristics including rms, height, correlation length, and correlation functions, and incidence angles from 20° to 60°. These parameters are summarized in Table II. The commonly used correlation functions are the gauss and exponential functions. The gauss function generally describes a random rough surface with a single dominant scale, where the exponential correlation function represents a multiscale random rough surface. As shown in [23], the correlation functions of most natural random rough surfaces are generally between the gauss and exponential functions. Our simulated database should be valid for most natural random rough surfaces. Surfaces with row patterns are outside the scope of this study and need to be studied in the future.

Through our evaluation of the effects of surface properties on microwave emissivity at different polarizations and incidence angles, we found that several important characteristics of surface roughness effects were not explained or addressed in the current semiempirical models. These include the following.

TABLE II
Soil Moisture and Surface Roughness Parameters Used in Simulations

Soil Parameters	Minimum	Maximum	Interval	Unit
Moisture	2.0	44	2	% by volume
RMS height	0.25	3.5	0.25	cm
Correlation length	2.5	30	2.5	cm
Incidence angle	20	60	1	degree
Correlation functions	Exponential , 1.5 power, and Gaussian			

- Roughness effects on the surface effective reflectivity differ at different incidence angles and polarizations for the same surface roughness parameters (ks, kl, and the correlation functions) in both the magnitudes and directions that increase or decrease the surface effective reflectivity.
- Surface roughness has a significant effect on the V/H ratio measurements.

Fig. 2 shows the IEM model simulated effective surface reflectivity (y axis) for all combinations of surface roughness and soil moisture parameters listed in Table II versus the corresponding flat-surface reflectivity (x axis) for H (top) and V (bottom) polarizations at 30° (left) and 50° (right), respectively. The departing of the effective reflectivity from the straight diagonal 1:1 line in Fig. 2 represents the effect of surface roughness. For H polarization, the effects of surface roughness always reduce the reflected energy or increase the emission in comparison with that from a flat surface, although the magnitudes are different at different incidence angles. This is a commonly understood phenomenon. However, the effects of surface roughness on V polarization significantly change in both magnitude and direction at different incidence angles as

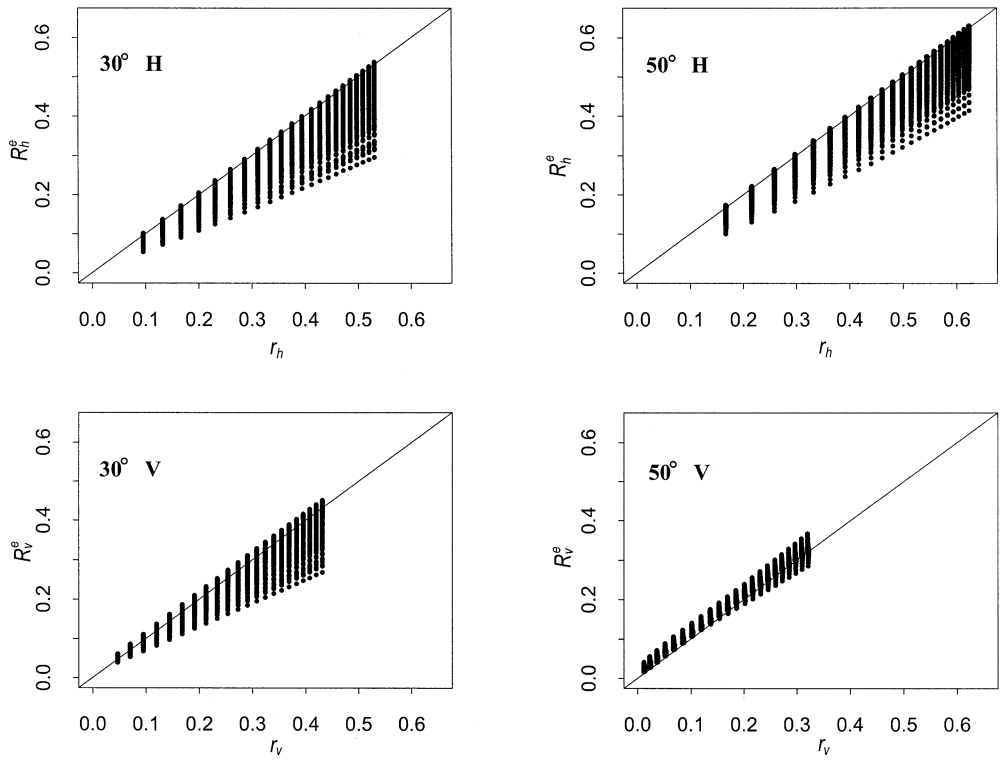

Fig. 2. IEM model simulated effective surface reflectivity (y axis) for all combinations of surface roughness and soil moisture parameters listed in Table II versus the corresponding Fresnel reflectivity (x axis) for H (top) and V (bottom) polarizations at 30° (left) and 50° (right), respectively.

shown in the bottom of Fig. 2. At 30°, the effect of the surface roughness has the same direction as H polarization despite different magnitudes for most of the simulated cases. Surface effective reflectivity is reduced at both polarizations. In contrast to 30°, the effect of roughness at 50° for the two polarizations is different in magnitude and direction for most cases. For vertical polarization, the roughness actually increases the surface effective reflectivity or decreases the emission for most cases compared to that of a flat surface.

From (1)–(3), we can see that the surface reflectivity mainly consists of two components, namely, coherent and incoherent. The coherent component is only affected by θ (the incidence angle) and ks (the normalized surface rms height) for a given dielectric constant. The coherent component always decreases as the surface roughness ks increases at a given incidence angle, and it decreases as the incidence angle decreases for a given ks. The reflectivity of the coherent component for H polarization is always greater than that for V polarization. Especially when it reaches the Brewster angle, the coherent component of V polarization can be very small or approaches zero. It is a dominant component at L-band especially at large incidence angles and H polarization.

The noncoherent component is a function of θ, ks, kl, and the form of the surface correlation function. It always increases as the surface roughness increases. At H polarization, the noncoherent term is generally smaller than that for V polarization. The overall effect of surface roughness is actually a combined effect from these two components: one decreases, and the other increases as the roughness changes. As a result, the total reflected energy may have two outcomes when comparing rough to flat surfaces. If the reduction in the coherent component of the reflected energy is greater than the increase in the noncoherent scattering, then surface roughness will appear to reduce the effective reflectivity. This represents all cases for H polarization at all incidence angles. However, when the amount of the reduced coherent component in the reflected energy is less than the increase in the noncoherent scattering, then surface roughness will appear to increase the effective reflectivity. This can occur in V polarization due to the effect of the Brewster angle in the coherent component. To explain this phenomena, we show each scattering component of (1) as a function of the surface rms height for H polarization (top) and V polarization (bottom) at 30° (left) and 50° (right) in Fig. 3. The data were simulated with soil moisture of 20% and a correlation length of 15 cm with a gauss correlation function. The solid line is the total surface effective reflectivity. The $+$ and * are for the coherent and noncoherent reflection components. In Fig. 3 for H polarization (top) at both incidence angles, the rate of the coherent reflectivity decreases faster than the rate of the noncoherent reflectivity increases when the surface roughness s increases. Therefore, the total reflectivity decreases as $s$increases. For V polarization at 30° in Fig. 3 (bottom left), the total reflectivity has almost no change for all values of s because the rate change in both coherent and noncoherent components is similar. For V polarization at 50° (bottom right in Fig. 3), however, the amount of the reflected energy in the coherent component decreases slower than that in the noncoherent component increases. As a result, surface roughness can cause an increase in the surface effective reflectivity at V polarization that strongly depends on the incidence angle and the surface roughness properties. In our simulated database, the percentages of the IEM-simulated effective reflectivity at V polarization that are greater than their

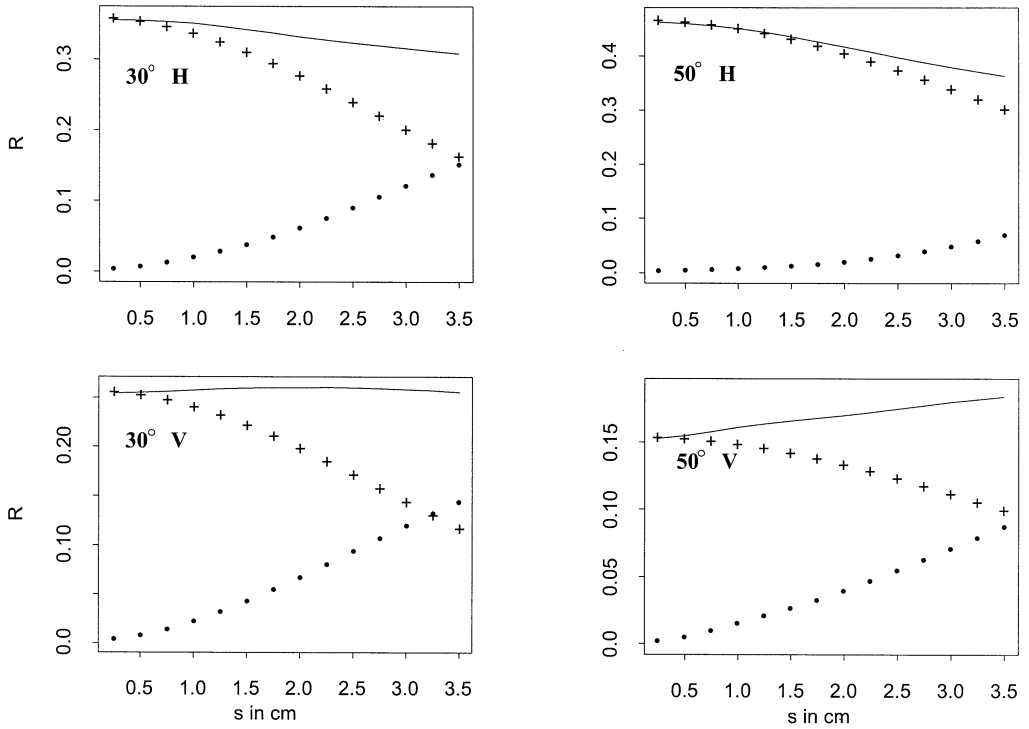

Fig. 3. IEM model simulated scattering components as a function of s for H polarization (top) and V polarization (bottom) at 30° (left) and 50° (right) with the gauss correlation function for soil moisture 20% and correlation length 15 cm. The solid line is the total surface effective reflectivity. The $+$ and $*$ are for the coherent and noncoherent reflection components.

corresponding Fresnel reflectivity in the total simulated data increased as the incidence angle increased. This percentage is quite small at small incidence angles (with only 8% at 20°), while all of the simulated V polarization data are larger than their corresponding Fresnel reflectivity at 55° or higher. This is in contrast to the current semiempirical models. These models predict that increased surface roughness results in a decrease in the effective reflectivity or an increase in the emitted energy for both V and H polarizations when compared with a flat surface. We noticed that the Q/H model could predict an increase of the effective reflectivity in V polarization under the arbitrary roughness condition with large Q and H ≈ 1. However, it has the similar prediction as the other semiempirical models [14]–[17] when using the physically based surface roughness parameter (rms height) [12]. This is because the H parameter is a dominant roughness control factor.

Furthermore, to demonstrate the effects of surface roughness on the R_v^e/R_h^e ratio measurements, we show the IEM model simulated ratio of R_v^e/R_h^e at 30° for rough surfaces (y axis) versus r_v/r_h for flat surfaces in Fig. 4(A). If the roughness effects at V and H polarizations had the same magnitude and direction for any given combination of surface roughness parameters (ks, kl, and correlation functions), the R_v^e/R_h^e ratio measurement could cancel out the roughness effect. In this case, the ratio of R_v^e/R_h^e might be expected to be highly correlated with the flat-surface reflectivity ratio r_v/r_h. However, the results show that the roughness has a significant impact on the effective reflectivity R_v^e/R_h^e ratio measurements. It indicates that the effects of the surface roughness at different polarizations have different magnitudes even though they have the same direction. Fig. 4(B) shows the relationship of R_v^e/r_v (x axis) and

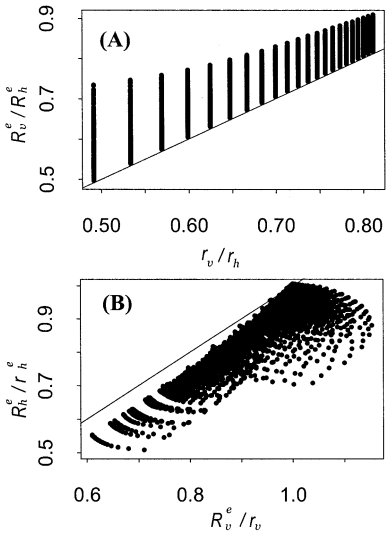

Fig. 4. (A) R_v^e/R_h^e (y axis) versus r_v/r_h (x axis) at 30° incidence and (B) the R_v^e/r_v (x axis) versus R_h^e/r_h (y axis).

R_h^e/r_h (y axis). The R_p^e/r_p can be considered here as a roughness correction factor for polarization p. Values that depart from one are due to the surface roughness effect, with larger departures indicating larger roughness effects. Since R_v^e/r_v is always greater than or equal to R_h^e/r_h, this indicates that the effect of surface roughness is significantly different at different polarizations and that the polarization ratio is greatly affected by surface roughness. In our simulated database, $R_v^e/R_h^e \geq r_v/r_h$ at all incidence angles. Therefore, this must be considered in both the surface effective reflectivity model and the inversion algorithm development.

TABLE III
COEFFICIENTS IN (7) FOR CALCULATING A_p ON TOP AND B_p AT BOTTOM IN (5)

Coefficient	e	g	h	Coefficient	e	g	h
a(V,p=1,2)	2.2732	-0.0381	-2.0096	a(V,p=3)	3.6497	-5.9528	2.5683
b(V,p=1,2)	2.1929	0.4262	-0.6729	b(V,p=3)	2.2630	0.4594	-0.8072
c(V,p=1,2)	-2.2287	-0.4087	1.9037	c(V,p=3)	-2.8358	0.0190	2.1056
d(V,p=1)	-0.0045	0	0	d(V,p=3)	-0.0942	-1.1369	1.3275
d(V,p=2)	-0.0799	-0.0469	0.1765	d(H,p=2)	-0.1095	0.1435	-0.0350
a(H,p=1,2)	2.3681	-0.6051	-1.3164	a(H,p=3)	3.2371	-4.2414	0.7546
b(H,p=1,2)	2.2634	0.0195	-0.1638	b(H,p=3)	2.3899	-0.0937	-0.1543
c(H,p=1,2)	-2.3856	0.4520	0.9944	c(H,p=3)	-3.0082	0.8868	1.0937
d(H,p=1)	-0.0030	0	0	d(H,p=3)	-0.3245	-0.1541	0.2851

Coefficient	e	g	h	Coefficient	e	g	h
a(V,p=1,2)	-0.7417	3.0402	-3.3258	a(V,p=3)	-0.5864	2.5499	-3.1846
b(V,p=1,2)	-0.0993	-0.3694	0.3989	b(V,p=3)	-0.0869	0.2757	-0.3008
c(V,p=1,2)	0.3090187	-1.2325	1.1855	c(V,p=3)	0.3271	-1.2145	1.1665
d(V,p=1)	-0.0058	0	0	d(V,p=3)	0.1031	-0.3511	0.1348
d(V,p=2)	0.0101	-0.0671	0.0280	d(H,p=2)	0.0077	0.0203	-0.0005
a(H,p=1,2)	0.1291	-0.6484	0.7685	a(H,p=3)	0.1184	-0.7560	1.1571
b(H,p=1,2)	0.0191	-0.1139	0.0473	b(H,p=3)	-0.0101	-0.0086	-0.0328
c(H,p=1,2)	-0.1445	0.6046	-0.3569	c(H,p=3)	-0.0677	0.3333	-0.1384
d(H,p=1)	0.0054	0	0	d(H,p=3)	-0.0033	0.0209	0.1187

IV. PARAMETERIZED IEM MODEL

Using the IEM-simulated database, we developed a simple model for the parameterization of surface roughness effects that are convenient and easy to use in relating the ground surface properties measurements to the emission signal directly without significant computational efforts. We found that the surface effective reflectivity could be described as

$$R_p^e = R_p^{\mathrm{coh}} + A_p \cdot r_p^{B_p} \tag{4}$$

where R_p^{coh} is given in (3). A_p and B_p are roughness parameters that will depend on the polarization, incidence angle, surface rms height, correlation length, and the type of the correlation function. They represent an overall effect of the surface roughness. We selected the roughness parameter B_p because the log–log form is generally better than the linear relation form for a wide range of incidence angles in presenting the relationship between the noncoherent surface reflectivity and the Fresnel reflectivity. The roughness parameters A_p and B_p can be calculated by a common form

$$A_p \text{ or } B_p = \exp(a(\theta,p,\rho) + b(\theta,p,\rho)\cdot\log(ks) + c(\theta,p,\rho)\cdot ks + d(\theta,p,\rho)\cdot W). \tag{5}$$

The coefficients a, b, c, and d depend on the incidence angle, polarization, and the type of the correlation function ρ, where $\rho = 1$ is Gaussian, $\rho = 2$ is 1.5-power, and $\rho = 3$ is exponential. They are determined through regression analyses using our IEM model simulated database. W is the surface roughness power spectrum, which is the Fourier transform of the correlation function ρ. For three commonly used correlation functions, it is given by [21]

$$W(\theta) = \begin{cases} 0.5\cdot(kl)^2\cdot\exp\left(-(\sin(\theta)\cdot kl)^2\right) & \text{gauss} \\ (kl)^2\cdot\exp(-2\cdot\sin(\theta)\cdot kl) & \text{1.5-power} \\ (kl)^2/\left(1+(2\sin(\theta)\cdot kl)^2\right)^{1.5} & \text{exponential.} \end{cases} \tag{6}$$

Furthermore, the angular dependence of the coefficients a, b, c, and d for a given polarization and correlation function can be described by a second-order function

$$a,b,c,d(\theta,p,\rho) = e(p,\rho) + g(p,\rho)\cdot\theta + h(p,\rho)\cdot\theta^2 \tag{7}$$

where θ is in radians. Table III gives the coefficients of e, g, and h for different polarizations and types of correlation functions. It is found that 1) the coefficients a, b, and c from the gauss and 1.5-power correlation functions have no significant difference, but they differed from those of the exponential correlation function, and 2) the d coefficient from the gauss correlation function has no angular dependence and is a constant.

Now, we can calculate the surface effective reflectivity by the following steps.

- Step 1) Calculate the coefficients a, b, c, and d for a given incidence θ, polarization p, and correlation function ρ using (7) and the coefficients of e, g, and h from Table III.
- Step 2) Calculate the coefficients A_p and B_p from the coefficients a, b, c, and d using (5).
- Step 3) Then use (4) to calculate the surface effective reflectivity R_p^e.

Fig. 5 shows the rmse as a function of incidence angle of results from this simplified model compared with that directly calculated by the IEM model. In Fig. 5, the letters V and H represent V and H polarizations, respectively. The parameterized model (4) has an accuracy (rmse) better than 0.01 for V polarization at all incidence angles, with the best accuracy of 0.0035 around 40°. For H polarization, the accuracy increases as the incidence angle increases, with the worst accuracy of 0.011 at 20° and the best accuracy of 0.0028 at 60°. These results indicate that this parameterized model can be used in place of IEM model predictions over a wide range of surface roughness conditions.

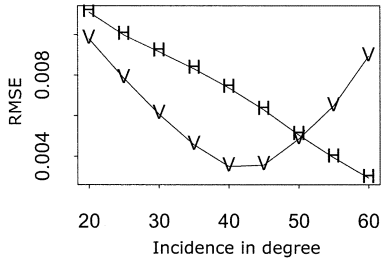

Fig. 5. RMSE (y axis) of the parameterized model (4) in comparison with the IEM model predications at different incidence angles (x axis).

V. Inversion Model Development

In the single-polarization inversion technique described in [1] and [2], the surface roughness correction factor must be determined from other data sources in order to estimate soil moisture. Dual-polarization measurements, however, provide an opportunity to minimize surface roughness effects and to estimate soil moisture directly for bare soils. Considering that surface roughness parameters (ks, kl, and the form of the correlation function) affect the surface emission signals, it is unrealistic to solve for all unknowns from only limited observations, given that there are only two microwave measurements available (V and H polarizations). The task is to reduce the dimensionality of the problem by eliminating some of the surface roughness parameters. This may be possible if they are highly correlated with each other at the different polarizations. If they are highly correlated, it would be possible to minimize the effects of the surface roughness so that soil moisture could be estimated.

Our algorithm development was based on the optimization scheme techniques to minimize the surface roughness effects using our simulated database that covered a wide range of the surface roughness and soil moisture conditions at each incidence angle. We evaluated the different combinations or forms from R_v^e and R_h^e in terms of minimizing the surface roughness effects through statistical regression analyses. It is found that the inversion model to estimate soil moisture using dual-polarization V and H measurements can be written as

$$\frac{r_v(\theta)}{r_h(\theta)} = \exp\left(A(\theta) + B(\theta)\cdot\log(R_v^e(\theta)) + C(\theta)\cdot\log(R_h^e(\theta)) + D(\theta)\cdot R_v^e(\theta)/R_h^e(\theta)\right). \quad (8)$$

This model uses the different weight on the surface effective reflectivity measurements at different polarizations to minimize the surface roughness effects so that the response of the measurements to the Fresnel reflectivity ratio [left side of (8)] can be estimated. The parameters A, B, C, and D are determined through the statistical optimization by the least square fitting analyses from our IEM model simulated database. These parameters are dependent only on incidence angle. Since the angular dependence of these coefficients can be described by a second-order function, they can be determined using (7). Table IV gives the parameters e, g, and h that are needed to calculate the coefficients A, B, C, and D in (8). Furthermore, the surface dielectric properties or soil moisture (with known soil texture information) can be derived from the Fresnel reflectivity ratio, since it only depends on the surface dielectric property and incidence angle.

TABLE IV
THE COEFFICIENTS USING (7) TO CALCULATE THE COEFFICIENTS A, B, C, AND D IN (8)

Coefficient	e	g	h
A	-2.1709	2.2257	0.5635
B	-2.8503	6.2650	-2.8191
C	4.4976	-12.6343	9.4187
D	1.8908	-1.2533	-1.2343

Fig. 6(A) shows the estimated volumetric soil moisture in percent at 40° (y axis) by (8) versus its corresponding input soil moisture (x axis) that was used to simulate the surface effective reflectivity using the IEM model. The rmse is 0.83. Fig. 6(B) (solid line) shows the accuracies in rmse in percent as a function of incidence angles from 20° to 60°. In terms of general behavior, the inversion accuracy is 1.68% at 20°. The rmse reduces as the incidence angle increases (up to a point). The best accuracy can be seen at 45° with 0.55% rmse. As the incidence angle further increases, the rmse starts to increase with the worst case 2.53% at 60° incidence angle. Based on comparisons to the IEM-simulated data, the inversion model is quite accurate.

In order to evaluate the behavior of the inversion model (8) on estimation of soil moisture, we performed sensitivity tests by introducing the absolute error and relative error in the IEM-simulated surface effective reflectivity. The effect of the absolute error was evaluated from adding or subtracting an error in both V and H polarizations simultaneously. The relative error was introduced from $\pm$ error/2 to one polarization and that with opposite sign to the other polarization. Fig. 6(C) shows the effects of the absolute and relative errors on the volumetric soil moisture in percent estimation by (8) using the IEM-simulated data as a function of the incidence angle in degrees. The solid line represents the accuracy using the IEM-simulated data. The angular behaviors, due to the absolute (adding 0.015) and relative (adding 0.0075 to V polarization and subtracting 0.0075 from H polarization) errors, for (8) are shown with dotted and dashed lines, respectively. The results show that the algorithm is sensitive at small incidence angles less than 25° and insensitive at incidence angles larger than 30° for relative errors. This is because there is a smaller dynamic range for the differences between R_v^e and R_h^e at small incidence angles than at large incidence angles. For the absolute errors, it is sensitive at larger incidence angles but less sensitive at small incidence angles. At incidence angles less than 50°, the rmse errors are only slightly above 2%. Fig. 6 (right plot) shows the errors in estimating volumetric soil moisture in percent for (8) due to introducing the absolute and relative errors to the IEM-simulated data at 40° incidence angle. The bottom x axis is the absolute error that was introduced to the IEM-simulated R_p^e either through subtraction (negative) or addition (positive). The relative errors (top x axis) were introduced with half of the absolute errors and same sign to the V polarization but with the opposite sign to the H polarization. The test results due to the absolute and relative errors of the average errors (the input moisture—the estimated moisture) are represented by the dotted and dashed lines, and those corresponding to rmse are shown by * and +, respectively. The average errors or the bias of the inversion model resulting from the absolute error behave in a similar manner as the reflectivity

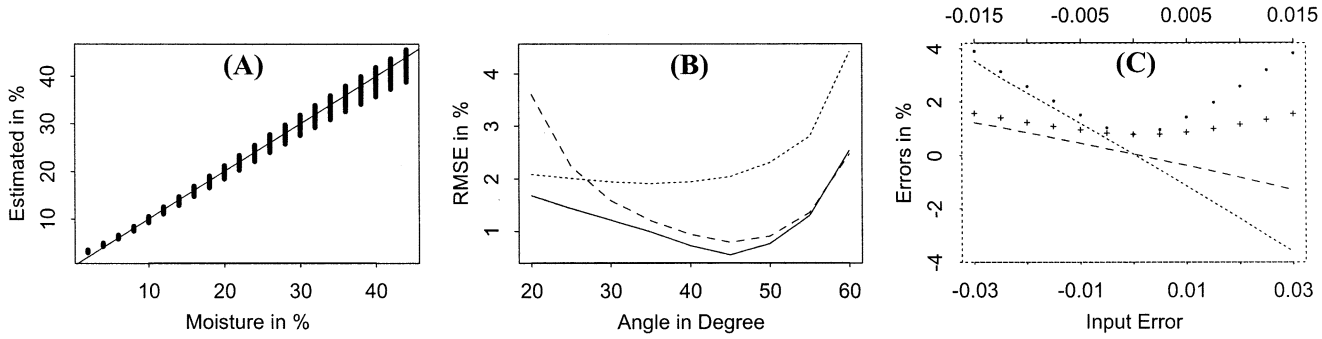

Fig. 6. (A) Estimated volumetric soil moisture in percent at 40° (y axis) by (8) versus its corresponding input soil moisture (x axis) using the IEM model. (B) RMSE on the estimation of volumetric soil moisture in percent (y axis) of the inversion model using all IEM-simulated data (solid line), adding 0.015 absolute (dotted line) and relative (dashed line) errors to the simulated data as a function of incidence angle (x axis in degrees). (C) Estimation errors of soil moisture in percent (y axis) at 40° with the errors (x axis) introduced to the simulated data. The labels of the x axis at the bottom and top indicate the absolute and relative errors, respectively. The biases resulted from the absolute error (dotted line) and the relative (dashed line) error, and the corresponding rmse errors are represented as * and $+$, respectively.

response to soil moisture. The negative absolute errors resulted in the underestimation of soil moisture while the positive ones caused overestimation. A 3% absolute error could result in an average of 4% error in soil moisture estimation. On the other hand, the relative error has much less impact on the algorithm performance at a 40° incidence angle. The resulting rmse and average errors in estimating soil moisture were all less than 2%. It is interesting to notice that the average errors followed the errors that were introduced to V polarization. The negative errors in V polarization resulted in underestimation, and the positive ones caused overestimation. It can be seen that the rmse and the bias had similar magnitudes, indicating that the introduced absolute and relative errors mainly result in a biased estimation of soil moisture.

VI. Validation With Field Experimental Data

A truck-mounted microwave radiometer experiment dataset consisting of L-band (1.4 GHz) observations made over several bare-surface test sites at Beltsville, MD during a four-year period (1979–1982) [24]–[27] was used to test the algorithm. The radiometer used in these past experiments was a dual-polarized Dicke radiometer that measured thermal microwave emission in both vertical and horizontal polarizations almost simultaneously. Calibration of this system was verified daily by measuring two targets of known brightness temperature: the cold sky and a microwave-absorbing material (Eccosorb). At the beginning and end of the measurement season, the system was also calibrated over a pond of fresh water at a known temperature. The reported calibration accuracy is about $\pm$ 3 K. The ground truth on the vertical profiles of soil moisture and temperature as well as soil bulk density and texture were acquired simultaneously with the microwave radiometer measurements. The surface roughness condition for the 1979–1980s sites was visually interpreted as smooth surface [24], [25]. In 1981's experiment, the surface roughness was measured at three study sites with the surface rms height 0.21, 0.73, and 2.45 cm, respectively [13]. But no surface roughness condition was reported in 1982's experiment [27]. These experimental data have been used to study the effects of soil texture, surface roughness, and vegetation cover on the remote sensing of soil moisture content by microwave radiometers and are well documented in [24]–[27].

In order to evaluate the accuracy of the soil moisture algorithm, the effects of the vertical distribution of soil moisture and temperature have to be taken into account. To do so, we first derived the effective soil temperature using a simple incoherent radiative transfer method [4]

$$T_s^e(\theta) = \int_{-\infty}^{0} T_s(z) \cdot F_{Np}(\varepsilon(z)) \cdot dz. \tag{9}$$

$T_s^e(\theta)$ is the soil "effective temperature." $T_s(z)$ is the soil temperature at the depth of z, and

$$F_{Np}(\varepsilon(z)) = \alpha(z) \cdot \exp\left(-\int_{z}^{0} \varepsilon(z') \cdot dz'\right) \tag{10}$$

is an approximation of the emitted energy from the depth z and normalized to an integral of unity. $\alpha(z)$ is the corresponding absorption coefficient at depth z and can be calculated by

$$a(z) = 2k\mathrm{Im}\left\{\sqrt{\varepsilon_r(z) - \sin^2\theta}\right\}. \tag{11}$$

ε_r is the relative dielectric constant. The surface effective reflectivity can then be derived from the measured brightness temperature as follows:

$$R_p^e(\theta) = 1 - T_{\mathrm{op}}(\theta)/T_s^e(\theta). \tag{12}$$

T_{op} is the instrument-observed brightness temperature. Equation (9) indicates that the effective soil temperature can be interpreted as a weighted mean temperature from the soil temperatures at the different depths and weighted by its corresponding normalized emitted energy. In a manner similar to this concept, we calculate the effective soil moisture SM

$$\mathrm{SM}(\theta) = \int_{-\infty}^{0} \mathrm{SM}(z) \cdot F_{Np}(\varepsilon(z)) \cdot dz. \tag{13}$$

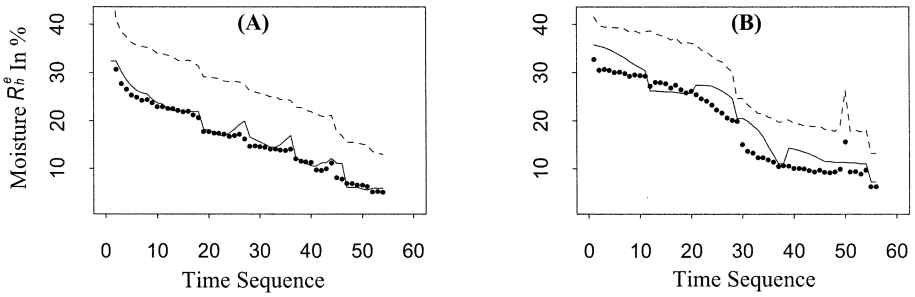

Fig. 7. Comparison of the estimated and measured ground soil moistures from the time-series measurements at 20° over two bare-surface test sites (A) E4 and (B) S4. The x axis is the time sequence in the observations. The solid line is the equivalent soil moisture. The dashed line is the surface effective reflectivity of H polarization measurements in percent. The dots are the estimated soil moisture by the algorithm.

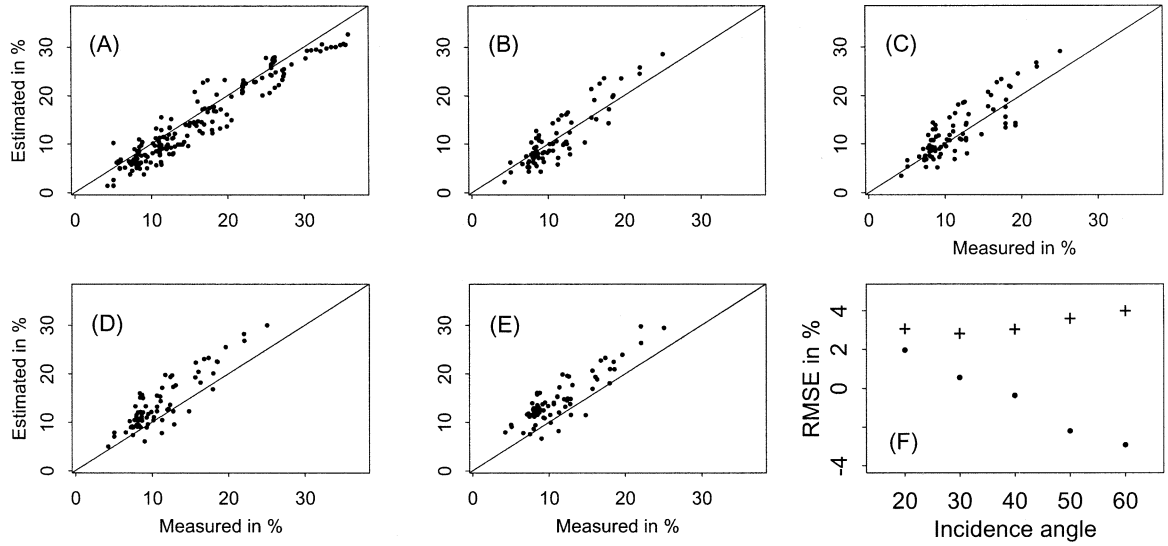

Fig. 8. Comparison of the estimated volumetric soil moisture (y axis) and measured ground volumetric soil moistures in percent (x axis) at Beltsville, MD during a four-year period from 1979 to 1982 for all bare-surface experiment data. (A)–(E) represent the test data from the incidence angles 20° to 60°, respectively. (F) shows the mean difference (bias) as $*$ and the corresponding rmse as $+$ between the measured and estimated volumetric soil moistures at each incidence angle.

Fig. 7(A) and (B) shows the comparison of the estimated and measured ground soil moistures from the time-series measurements at a 20° incidence angle during the 1982 experiment [27] over two bare-surface test sites E4 and S4, respectively. The x axis is the time sequence of the observations. The solid line is the equivalent soil moisture calculated using (13). The dashed line is the surface effective reflectivity of H polarization in percent calculated from the radiometer measurements using (9)–(12). The dots are the soil moisture estimated by the algorithm in (8). The experiment at site E4 was conducted over a ten-day period from August 2 to 11, 1982, and the experiment at site S4 covered an eight-day period from August 16 to 23, 1982. Most of the observations were made between 10 a.m. to 2 p.m. on each day. These two time-series measurements were conducted after rainfall events and represented a soil moisture dry-down cycle. The microwave sensor was fixed at a 20° incidence angle throughout the experiment. It provided stable measurements, since the measured footprint locations were not changed during the experiment each day. For site E4, the algorithm estimates were quite accurate with an rmse of 1.67% with a slight bias toward underestimation of soil moisture. The measured surface effective reflectivity (dashed line) and the measured (solid line) and estimated (dots) soil moisture all correspond reasonably well in both overall trend and diurnal variation.

For site S4, the measurements of surface effective reflectivity R_h^e did not mirror the diurnal fluctuation that was seen in soil moisture measurements, although the overall trend did capture the moisture dry-down condition. Since the estimated soil moisture is based solely on the instrument measurements, the algorithm clearly underestimated the soil moisture with an rmse of 3.4%. Ground sampling of soil moisture and temperature was made at only two depths: 0–2 cm and 2–4 cm. One possible reason why the brightness temperature did not respond to diurnal fluctuation of the measured soil moisture was that the sensor might be responding to the temperature and soil moisture in a layer deeper than the sampled layer. This deeper layer did not exhibit such a strong diurnal pattern.

Fig. 8(A)–(E) shows the comparison of estimated and measured volumetric soil moisture for all bare-surface measurement sites from 1979 to 1982. The number of the observations is 187, 76, 85, 75, and 76 for an incidence angle from 20° to 60°, re-

spectively. Fig. 8(F) shows the mean difference (bias) and the corresponding rmse between the measured and estimated volumetric soil moistures at each incidence angle. The new soil moisture retrieval algorithm performance underestimates soil moisture with the most cases at 20° with a mean error of 1.8%. As the incidence angle increases to 30° and 40°, there is less bias with a bias of 0.4% and −0.5%. However, as the incidence angles increase to 50° and 60°, overestimation of soil moisture increases with biases of −2.3% and −3.0%, respectively. This clear trend in the algorithm performance might be the result from the two possible reasons. The first one might be caused by the effect of the antenna pattern of the radiometer. The actually sampled footprints on the ground might vary in size and location at the different incidence angles. The other might be due to the bias trend in the algorithm for certain roughness conditions. This is because the algorithm is developed and has no bias under a very wide range of the surface roughness conditions. However, the algorithm can have the bias for the specific roughness conditions from a few experiment sites. For the algorithm (8), except for 60°, all rmses are within or about 3% for incidence angles from 20° to 50°, with the best estimation at 30° (2.6%).

VII. Conclusion

Understanding the effects of surface roughness on microwave emission and developing quantitative bare-surface soil moisture retrieval algorithms are essential to many applications of geophysical properties in complex earth terrain by microwave remote sensing. In this study, we first validated the IEM model with a highly accurate but complex 3-D Monte Carlo model. A comparison showed that the IEM model slightly overestimates the emissivity for V polarization with rmses of 0.008 and 0.013 at 40° and 50° incidence angles, respectively. For H polarization, the errors were more random with rmses of 0.01 and 0.017 at 40° and 50°. The results indicate that the IEM model can be used to simulate the surface emission quite well for a wide range of surface roughness and conditions.

Then, we used an IEM model to simulate a database with a wide range of surface roughness and dielectric conditions. Using the IEM-simulated data, we demonstrated several important characteristics of surface roughness effects on microwave emission signals that were not incorporated in currently used surface effective reflectivity models. It was found that the effects of surface roughness on microwave emission signals at V and H polarization might be different in both magnitude and direction, depending on the incidence angle, surface roughness, and dielectric properties. The overall effect of surface roughness can be explained by the combined effects from two components: the coherent component that decreases as the surface roughness increases and the noncoherent component that increases as the roughness changes. As a result, the total reflected energy may have two outcomes when comparing rough and flat surfaces. If the amount of reduction in the coherent component of the reflected energy is greater than the increase in noncoherent scattering, surface roughness reduces the effective reflectivity. This represents all cases for H polarization at all incidence angles. However, when the amount of the reduction in the coherent component of the reflected energy is less than the increase in the noncoherent scattering, surface roughness actually increases the effective reflectivity. This only occurs in V polarization. As a result, the surface effective reflectivity in V polarization could be greater than its corresponding Fresnel reflectivity depending on the incidence angle, surface roughness, and dielectric properties. This also impacts roughness effects on the polarization ratio V/H measurements. These two important characteristics have been not incorporated in the currently available semiempirical surface effective reflectivity models.

We developed a surface effective reflectivity model for L-band (1.4 GHz) utilizing both V and H polarizations and three typical correlation functions (gaussian, 1.5-power, and exponential) by parameterizing the IEM model simulated data for a wide range of surface soil moisture and roughness properties. When compared to the IEM model simulated data, the parameterized model in (4) has the accuracy (rmse) better than 0.01 for V polarization at all incidence angles with the best accuracy (0.0035) at 40°. For H polarization, the accuracy increases as the incidence angle increases with the worst accuracy (0.011) at 20° and the best accuracy (0.0028) at 60°. These results indicate that the parameterized model can reproduce the IEM model predictions over a wide range of surface roughness conditions.

Using the IEM model simulated database for a wide range of surface soil moisture and roughness properties, we developed an inversion model that uses dual polarization measurements to minimize surface roughness effects and to estimate surface dielectric properties directly. For the IEM model simulated data, the algorithm in (8) has an accuracy of 1.68% at 20°. The accuracy increases as the incidence angle increases. The best accuracy can be seen at 45° with 0.55%. Validation of this inversion technique with ground microwave radiometer experiment data indicated that there was an overall trend for soil moisture underestimation in the algorithm performance. However, all rmses are within or about 3% for incidence angle between 20° and 50°.

References

[1] T. J. Jackson, D. E. LeVine, C. T. Swift, T. J. Schmugge, and F. R. Schiebe, "Large area mapping of soil moisture using the ESTAR passive microwave radiometer in Washita'92," *Remote Sens. Environ*, vol. 53, pp. 27–37, 1995.

[2] T. J. Jackson and D. E. LeVine, "Mapping surface soil moisture using an aircraft-based passive microwave instrument: Algorithm and example," *J. Hydrol.*, vol. 184, pp. 85–99, 1996.

[3] Y. H. Kerr and E. G. Njoku, "A semi-empirical model for interpreting microwave emission from semiarid land surfaces as seen from space," *IEEE Trans. Geosci. Remote Sensing*, vol. 28, pp. 384–393, Mar. 1990.

[4] E. G. Njoku and L.Li Li, "Retrieval of land surface parameters using passive microwave measurements at 6–18 GHz," *IEEE Trans. Geosci. Remote Sensing*, vol. 30, pp. 79–93, Mar. 1999.

[5] J. P. Wigneron, P. Waldteufel, A. Chanzy, J.-C. Calvet, and Y. Kerr, "Two-dimensional microwave interferometer retrieval capabilities over land surface (SMOS mission)," *Remote Sens. Environ.*, vol. 73, pp. 270–282, 2000.

[6] M. Owe, R. D. Jeu, and J. Walker, "A methodology for surface soil moisture and vegetation optical depth retrieval using the microwave polarization difference index," *IEEE Trans. Geosci. Remote Sensing*, vol. 39, pp. 1643–1654, Aug. 2001.

[7] S. Paloscia, G. Macelloni, E. Santi, and T. Koike, "A multifrequency algorithm for the retrieval of soil moisture on a large scale using microwave data from SMMR and SSM/I Satellite," *IEEE Trans. Geosci. Remote Sensing*, vol. 39, pp. 1655–1661, Aug. 2001.

[8] Y. H. Kerr, P. Waldteufel, J. P. Wigneron, J. M. Martinuzzi, J. Font, and M. Berger, "Soil moisture retrieval from space: The Soil Moisture and Ocean Salinity (SMOS) Mission," *IEEE Trans. Geosci. Remote Sensing*, vol. 39, pp. 1729–1735, Aug. 2001.

[9] E. G. Njoku, W. J. Wilson, S. H. Yueh, and Y. Rahmat-Samii, "A large-antenna microwave radiometer-scatterometer concept for ocean salinity and soil moisture sensing," *IEEE Trans. Geosci. Remote Sensing*, vol. 38, pp. 2645–2655, Nov. 2000.

[10] F. T. Ulaby, R. K. Moore, and A. K. Fung, *Radar Remote Sensing and Surface Scattering and Emission Theory*. Reading, MA: Addison-Wesley, 1982, vol. 2, Microwave Remote Sensing: Active and Passive.

[11] B. J. Choudhury, T. J. Schmugge, A. Chang, and R. W. Newton, "Effect of surface roughness on the microwave emission from soil," *J. Geophys. Res.*, vol. 84, no. C9, pp. 5699–5706, 1979.

[12] J. R. Wang and B. J. Choudhury, "Remote sensing of soil moisture content over bare fields at 1.4 GHz frequency," *J. Geophys. Res.*, vol. 86, pp. 5277–5282, 1981.

[13] J. R. Wang, P. E. O'Neill, T. J. Jackson, and E. T. Engman, "Multifrequency measurements of the effects of soil moisture, soil texture, and surface roughness," *IEEE Trans. Geosci. Remote Sensing*, vol. GE-21, pp. 44–51, Jan. 1983.

[14] U. Wegmüller and C. Mätzler, "Rough bare soil reflectivity model," *IEEE Trans. Geosci. Remote Sensing*, vol. 37, pp. 1391–1395, May 1999.

[15] T. Mo and T. J. Schmugge, "A parameterization of the effect of surface roughness on microwave emission," *IEEE Trans. Geosci. Remote Sensing*, vol. 25, pp. 47–54, Jan. 1987.

[16] S. S. Saatchi, E. G. Njoku, and U. Wegmüller, "Synergism of active and passive microwave data for estimating bare soil surface moisture, in passive microwave remote sensing of land–atmosphere interactions," in *Proc. ESA/NASA Int. Workshop*, 1995, pp. 205–224.

[17] J. P. Wigneron, L. Laguerre, and Y. H. Kerr, "A simple parameterization of the L-band microwave emission from rough agricultural soil," *IEEE Trans. Geosci. Remote Sensing*, vol. 39, pp. 1697–1707, Aug. 2001.

[18] Y. Oh, K. Sarabandi, and F. T. Ulaby, "An empirical model and inversion technique for radar scattering from bare soil surface," *IEEE Trans. Geosci. Remote Sensing*, vol. 30, pp. 370–381, Mar. 1992.

[19] L. Tsang, J. A. Kong, K. H. Ding, and C. O. Ao, *Scattering of Electromagnetic Waves*. New York: Wiley, 2001, vol. 2, Numerical Simulations.

[20] Q. Li, L. Tsang, J. C. Shi, and C. H. Chan, "Application of physics-based two-grid method and sparse matrix canonical grid method for numerical simulations of emissivities of soils with rough surfaces," *IEEE Trans. Geosci. Remote Sensing*, vol. 38, pp. 1635–1643, July 2000.

[21] A. K. Fung, *Microwave Scattering and Emission Models and Their Applications*. Norwood, MA: Artech House, 1994.

[22] T. D. Wu, K. S. Chen, J. Shi, and A. K. Fung, "A transition model for the reflection coefficient in surface scattering," *IEEE Trans. Geosci. Remote Sensing*, vol. 39, pp. 2040–2050, Sept. 2001.

[23] J. Shi, J. Wang, A. Hsu, P. O'Neill, and E. T. Engman, "Estimation of bare surface soil moisture and surface roughness parameters using L-band SAR image data," *IEEE Trans. Geosci. Remote Sensing*, vol. 35, pp. 1254–1266, Sept. 1997.

[24] J. Wang, J. Shiue, E. T. Engman, J. McMurtrey III, P. Lawless, T. Schmugge, T. Jackson, W. Gould, J. Fuchs, C. Calhoon, T. Carnahan, and E. Hirschmann, "Remote measurements of soil moisture by microwave radiometers at BARC Test Site I," NASA, NASA Tech. Memo. 80 720, 1980.

[25] J. Wang, P. O'Neill, E. T. Engman, J. McMurtrey III, P. Lawless, T. Schmugge, T. Jackson, W. Gould, J. Fuchs, and W. Glazer, "Microwave radiometer experiment of soil moisture sensing at BARC Test Site II," NASA, NASA Tech. Memo. 83 954, June 1982.

[26] J. Wang, T. Jackson, E. T. Engman, W. Gould, J. Fuchs, W. Glazer, P. O'Neill, T. Schmugge, and J. McMurtrey III, "Microwave radiometer experiment of soil moisture sensing at BARC Test Site during summer 1981," NASA, NASA Tech. Memo. 86 056, Jan. 1984.

[27] P. O'Neill, T. Jackson, B. Blanchard, R. van den Hoek, W. Gould, W. Glazer, J. McMurtrey III, and J. Wang, "The effects of vegetation and soil hydraulic properties on passive microwave sensing of soil moisture: Data report for the 1982 field experiments," NASA, NASA Tech. Memo. 85 106, Sept. 1983.

Jiancheng Shi (M'95–SM'02) received the B.A. degree from the University of Lanzhou, Lanzhou, China, in 1982, and the M.A. and Ph.D. degrees in geography from the University of California, Santa Barbara (UCSB), in 1987 and 1991, respectively.

He is currently with the Institute for Computational Earth System Sciences, UCSB, as a Research Scientist. His research interests are microwave modeling of snow and soil signatures, image processing and analysis, and inversion models for retrieving physical parameters from remote sensing data.

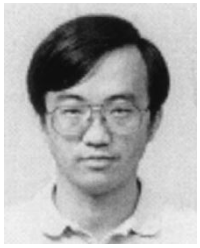

K. S. Chen (S'89–M'90–SM'98) received the B.S. degree from the National Taiwan Institute of Technology, Taipei, Taiwan, R.O.C., in 1985, and the M.S. and Ph.D. degrees from the University of Texas, Arlington, in 1987 and 1990, respectively, all in electrical engineering.

From 1985 to 19990, he was with the Wave Scattering Research Institute, University of Texas. In 1992, he joined the faculty of the Center for Space and Remote Sensing Research, National Central University, Chung-Li, Taiwan, R.O.C., where he is now a Professor and Director. He has joint appointments at the Institute of Space Sciences and Institute of Communication Engineering at the same university. His research activities involve in the areas of microwave remote sensing, image processing and analysis for satellite and aircraft remote sensing data, radio and microwave propagation, and scattering from terrain and ocean with applications to remote sensing and wireless communications. He has authored three book chapters, over 60 referred journal papers, and over 100 conference papers in the areas of remote sensing and wave scattering and propagation. He has been the Editor-in-Chief of *Journal of Photogrammetry and Remote Sensing* since 2001 and is on the Editorial Board of the *Journal of Electromagnetic Waves and Applications* and *Transactions of the Aeronautical and Astronautical Society of the Republic of China*. He serves as technical consultant at several national research agencies in areas of satellite remote sensing, radar, and radio techniques.

Dr. Chen was the recipient of the 1993 Young Scientist Award from the International Union of Radio Science (URSI) and has received numerous research awards from the National Science Council of Taiwan since 1993. He has been an Associate Editor of the IEEE TRANSACTIONS ON GEOSCIENCE AND REMOTE SENSING. In 2001, he was appointed as chairman of Commission F, Taipei, China of URSI. He is a member of the Electromagnetic Academy. He was a Technical Chairman of PIERS 1999, held in Taipei, Taiwan, R.O.C.

Qin Li received the B.S. and M.S. degrees in space physics from Wuhan University, Hubei, China, in 1985 and 1988, respectively, and the Ph.D. degree in electrical engineering from the University of Washington, Seattle, in 2000.

He is currently a Research Assistant Professor in the Department of Electrical Engineering, University of Washington. He has worked as a Post Graduate Researcher at the Institute for Computational Earth System Sciences, University of California, Santa Barbara.

Thomas J. Jackson (A'86–SM'96–F'02) received the Ph.D. degree in civil engineering from the University of Maryland, College Park, in 1976.

He is currently a Hydrologist with the USDA Agricultural Research Service Hydrology and Remote Sensing Laboratory, Beltsville, MD. His research involves the application and development of remote sensing technology in hydrology and agriculture. He has conducted research on the use of visible/near infrared satellite data for deriving land cover parameters used in hydrologic models and the use of an airborne laser profiler for measuring and monitoring soil erosion. His current research focuses on the use of passive microwave techniques in hydrology. These studies have ranged from small-scale controlled condition field experiments utilizing truck-mounted radiometers to large-scale multitemporal aircraft mapping.

Dr. Jackson received The Paper of the Year Award from the American Society of Agricultural Engineers for his paper "Airborne Laser Measurements of the Surface Topography of Simulated Concentrated Flow Gullies" in 1990, and the prize paper award for his "Diurnal Observations of Surface Soil Moisture Using Passive Microwave Radiometers" at the International Geoscience and Remote Sensing Symposium in 1994. He is a Fellow of the American Geophysical Union and currently serves on the Administrative Committee of the IEEE Geoscience and Remote Sensing Society.

Peggy E. O'Neill received the B.S. degree (summa cum laude with university honors) in geography from Northern Illinois University, Chicago, in 1976, and the M.A. degree in geography from the University of California, Santa Barbara, in 1979.

She has done postgraduate work in civil and environmental engineering through Cornell University, Ithaca, NY. Since 1980, she has been employed as a Physical Scientist in the Hydrological Sciences Branch, NASA Goddard Space Flight Center (GSFC), Greenbelt, MD, where she conducts research in soil moisture retrieval and land surface hydrology, primarily through microwave remote sensing techniques. She currently splits her time at GSFC between basic science research, new instrument technology development, and future space mission definition and planning.

Ms. O'Neill has been a recipient of NASA Outstanding Performance and Special Achievement Awards, a U.S. Department of Agriculture Certificate of Appreciation, and the 1994 IGARSS Symposium Prize Paper Award (as coauthor). She has served as a member of the organizing committee and technical program committee for several international scientific conferences. She is a member of the IEEE Geoscience and Remote Sensing Society, the American Geophysical Union, the American Meteorological Society (past member of Committee on Hydrology), and the International Association of Hydrological Sciences.

Leung Tsang (S'73–M'75–SM'85–F'90) was born in Hong Kong. He received the S.B., S.M., and the Ph.D. degrees from the Massachusetts Institute of Technology, Cambridge.

He is currently a Professor of electrical engineering at the University of Washington, Seattle, where he has taught since 1983. Starting September 2001, he has been on leave from the University of Washington and is a Professor Chair and Assistant Head of the Department of Electronic Engineering, the City University of Hong Kong. He is a coauthor of four books: *Theory of Microwave Remote Sensing* (New York: Wiley–Interscience, 1985), *Scattering of Electromagnetic Waves, Vol. 1: Theory and Applications* (New York: Wiley–Interscience, 2000), *Scattering of Electromagnetic Waves, Vol 2: Numerical Simulations* (New York: Wiley–Interscience, 2001), and *Scattering of Electromagnetic Waves, Vol 3: Advanced Topics* (New York: Wiley–Interscience, 2001). His current research interests include wave propagation in random media and rough surfaces, remote sensing, high-speed interconnects, computational electromagnetics, wireless communications, and optoelectronics.

Dr. Tsang was Editor-in-Chief of the IEEE TRANSACTIONS ON GEOSCIENCE AND REMOTE SENSING. He was the Technical Program Chairman of the 1994 IEEE Antennas and Propagation International Symposium and URSI Radio Science Meeting, the Technical Program Chairman of the 1995 Progress in Electromagnetics Research Symposium, and the General Chairman of the 1998 IEEE International Geoscience and Remote Sensing Symposium. He is a Fellow of the Optical Society of America and the recipient of the Outstanding Service Award of the IEEE Geoscience and Remote Sensing Society for 2000. He was also a recipient of the IEEE Third Millennium Medal in 2000. He is also an ADCOM member of the IEEE Geoscience and Remote Sensing Society.